

Influence of cell opening methods on organic solvent removal during pretreatment in lithium-ion battery recycling

Werner, D. M.; Mütze, T.; Peuker, U. A.;

Originally published:

October 2021

Waste Management and Research 40(2022)7, 1015-1026

DOI: <https://doi.org/10.1177/0734242X211053459>

Perma-Link to Publication Repository of HZDR:

<https://www.hzdr.de/publications/Publ-33685>

Release of the secondary publication
on the basis of the German Copyright Law § 38 Section 4.

Influence of cell opening methods on organic solvent removal during pretreatment in lithium-ion battery recycling

Denis Manuel Werner¹ , Thomas Mütze^{1,2} and Urs Alexander Peuker¹

¹Institute of Mechanical Process Engineering and Mineral Processing, TU Bergakademie Freiberg, Freiberg, Germany

²Helmholtz Institute Freiberg for Resource Technology (HIF), Freiberg, Germany

Corresponding author:

Denis Manuel Werner, Egastraße 2, 89446 Ziertheim, Germany.

Email: denis_manuel_werner@web.de

1 1 Introduction

2 Individual mobility, consumer electronics and electric energy storage are undergoing a
3 technological transformation due to the invention of Lithium ion batteries (LIBs). At the
4 moment, LIBs are applied already for most of the small- and medium-scale devices (Mossali et
5 al. 2020), and contain critical, high value and important key engineering metals such as cobalt
6 (Co), nickel (Ni), lithium (Li), copper (Cu) and aluminium (Al). The recycling of end of life
7 (EOL) LIBs is promoted by legislation, mainly because of local environmental and health risks
8 from hazardous materials, but also because of geostrategic and processing impacts as well as
9 economic and supply chain effects (Harper et al. 2019, Mossali et al. 2020, Pinegar et al. 2019b,
10 Rothermel et al. 2018).

11 However, the recycling of LIBs has also an environmental impact. In future, the production of
12 LIBs has to be performed in closed loops. Therefore, battery recycling processes have to follow
13 the developments in the LIB market and should be designed with the objective of compensating
14 their life cycle environmental impacts by increasing the overall recycling efficiency (RE)
15 (Kwade et al. 2018a).

16 One of the main challenges of LIB recycling is the batteries' hazard potential and the
17 corresponding depollution strategy. In this context, the depollution strategy significantly
18 influences the RE, the process design for a safe battery cell opening and the energy demand of
19 the whole process chain.

20 In order to evaluate and propose an overall disposal strategy regarding current and upcoming
21 LIB applications, designs and compositions, the present investigation focuses on different
22 methods for cell opening. The methods are combined with thermal drying to determine and
23 compare the overall solvent evaporation or each cell opening method and dismantling depths.
24 Consequently, technological and economical pre-treatment strategies for battery depollution
25 and safe cell opening are discussed.

26 2 Recycling of EOL LIBs

27 2.1 Lithium-ion batteries

28 2.1.1 Design and composition

29 In principle, the functional unit of a LIB consists of a negative electrode (anode) of graphite or
30 amorphous carbon compounds and a positive electrode (cathode) of a layered metal oxide. The
31 layered oxide contains Li in combination with Ni, Co, Al and/or manganese (Mn) individually
32 (LCO, LMO, LNO) or with different stoichiometry x , y and z on one hand ($N_xC_yA_z$, $N_x(M_y)C_z$)
33 or iron phosphate (LFP) on the other (Zhao et al. 2019). These active materials are coated on
34 an Al foil for the cathode and a Cu foil for the anode.

35 PVDF as well as carboxymethyl cellulose (CMC) combined with styrene-butadiene-rubber
36 (SBR) are “state of the art” binders for cathodes and anodes, respectively (Korthauer 2019,
37 Kwade et al. 2018b, Zhao et al. 2019). The binder acts as an adhesive for the coating material
38 itself connecting it with the current collector foils. Carbon black is added as a conducting
39 additive. Furthermore, petroleum coke, carbon fibre, pyrolysis carbon, glass carbon and carbon
40 black may be added (Kwade et al. 2018b, Zhao et al. 2019).

41 A porous plastic foil, the so-called separator, separates both electrodes. The pores of electrodes
42 and separator foil are filled with an ion-conducting electrolyte. The electrolyte is a high-purity
43 multi-component mixture of organic solvents, conductive salt and further additives. Ethylene
44 carbonate (EC), dimethyl carbonate (DMC), ethyl methyl carbonate (EMC), and diethyl
45 carbonate (DEC) are the most commonly used organic solvents. DMC, EMC, and DEC are light
46 boiling components with the boiling temperatures 90 °C, 107 °C and 127 °C respectively at
47 ambient pressure. In contrast, the high boiling solvent EC boils at temperatures of 248 °C
48 (Stehmann et al. 2018). Lithium hexafluorophosphate ($LiPF_6$) is almost exclusively used with
49 as conductive salt in commercial LIBs (Yang et al. 2006).

50 The functional unit of electrodes and separator is piled or winded during cell assembling. As a
51 result, the electrode-separator assembly forms stacks, or round as well as flat jelly rolls

52 (winding). The form of the functional unit determines the soft case pouch or hard case
53 cylindrical and prismatic cell type, respectively (Korthauer 2019, Kwade et al. 2018b).
54 Together, the functional unit and the hermetically sealed housing form the battery cell. Most of
55 today's cells exhibit metal-based housing and packaging material. The housing contains further
56 electrical connections, protection foils and functional components. Moreover, safety elements
57 on cell level, such as burst membrane, overcharging protection components, and fuses, are
58 added.

59 The cells as such are often connected in series or parallel. They form on the one hand a single
60 block or on the other hand a module as subunit of a larger battery system (Korthauer 2013,
61 Werner et al. 2020). Further peripheral functional and material components can be found on
62 module or system level, such as battery management system, cooling, packaging, electronic and
63 electric parts. As a general trend, all of the components are rising in complexity. Since cell
64 manufacturers use their individual formulations (Zhao et al. 2019), the battery functional
65 components, cells, modules as well as systems show a broad variety in used materials (Kwade
66 et al. 2018b) and thus, overall material composition (Arnberger et al. 2012, Chen et al. 2019,
67 Gaines et al. 2011, Georgi-Maschler et al. 2012, Kwade et al. 2018a, Kwade et al. 2018b,
68 Mossali et al. 2020, Wang et al. 2016, Weyhe 2008, Wuschke 2018).

69 2.1.2 Hazard potential

70 All LIBs have hazard potentials due to their voltage and state of charge as well as due to their
71 hazardous and reactive components. At the end of their lifetime, the hazard potentials of EOL-
72 LIBs can be summarized as electrical, chemical, and thermal hazards (Rahimzei 2017). The
73 hazard potentials interact with one another (Elwert et al. 2018, Gama 2014, Werner et al. 2020).
74 Particularly, the components of the electrolyte require special care. The organic solvents
75 potentially cause fire and explosion under special conditions (Hanisch et al. 2015, Wuschke
76 2018). Moreover, their hygroscopic properties promote corrosion (Kwade et al. 2018a). The
77 conductive salt exhibits only limited chemical and thermal stability. During battery lifetime,

78 and especially under abuse conditions or in worst-case scenarios, flammable and toxic gases
79 are generated as reaction or decomposition products. As a consequence of that, fire and several
80 chemical reactions occur before, during and after battery cell liberation (Korthauer 2019, van
81 Pels 2020).

82 2.2 Waste management

83 2.2.1 Complex waste

84 EOL-LIBs accumulate as unwanted production residues, but mainly as consumer residues
85 either during or after the end of their use period. EOL-LIBs are future and highly complex waste
86 with increasing complexity from the functional unit to the whole battery system (Pomberger et
87 al. 2014, Rudolph 1999). Consequently, reverse production in terms of automated disassembly
88 only could be realised at major expense by addressing the individual battery types and designs.
89 The great inhomogeneity in structure and composition as well as the problematic ingredients of
90 LIBs are challenging and require in high flexibility for disposal and recycling process design
91 (Wegener et al. 2014).

92 2.2.2 Recycling chain and technologies

93 The recycling chain for LIBs consists of four process stages with two unit operations each
94 (Martens et al. 2016, Werner et al. 2020). In the preparation stage (1), the batteries are usually
95 collected (1.1) either separately or mixed according to the battery type. After collection, the
96 batteries are sometimes if technologically possible sorted (1.2) with respect to either battery
97 type (LIB, alkaline battery, Ni-metal hydride battery, lead-acid battery etc.), LIB chemistry
98 (LCO, LMO, LFP, NMC), or even LIB active material ($N_1M_1C_1$, $N_6M_2C_2$, $N_8M_1C_1$). During
99 the subsequent pretreatment (2), the batteries are dismantled (2.1) to defined dismantling
100 depths. Also, the batteries are depolluted (2.2) regarding critical or hazardous components, or
101 material conditions for the subsequent processes. The aim of the processing stage (3) is to
102 liberate (3.1) the individual components or materials in order to separate (3.2) them physically

103 into defined concentrates. The refining of these concentrates occurs finally within the
104 metallurgical treatment (4) using extraction (4.1) and recovery processes (4.2).

105 The RE of a process was established within recycling efficiency ordinance (EU) 493/2012 to
106 quantify the usage of secondary (raw) materials for battery waste management and applied
107 technologies. The RE is obtained by relating the cumulative mass of recovered secondary (raw)
108 materials (output fractions) to the mass of batteries fed into the process (input/feed fractions)
109 (Tytgat 2013).

110 The industrial recycling technologies for EOL-LIBs can be clustered to three process routes:
111 low, medium, and high temperature route. The classification depends on the used temperature
112 to depollute the batteries. The temperature influences the corresponding effort for preparation
113 and processing, and overall RE (Werner et al. 2020). However, a high RE is reached only at the
114 expense of special safety strategies for a secured process design. That includes the process
115 medium and procedure for LIB system dismantling and liberation.

116 2.3 Dismantling

117 Disassembly of waste products conditions and reduces the feed material for further processing
118 (Schwarz et al. 2018). Especially, functional components or reusable assemblies can be
119 obtained for second-life applications (Harper et al. 2019, Idjis et al. 2013). Moreover,
120 assemblies or components that can be fed to established recycling routes increase the overall
121 RE (Elwert et al. 2018, Li et al. 2019, Wuschke et al. 2016). These materials decrease the
122 complexity of down-stream liberation and separation as well as refining processes (Schwarz et
123 al. 2018). The importance of dismantling strategies regarding their impact on the subsequent
124 processing are rarely discussed for EOL-LIB recycling. Therefore, our contribution focusses on
125 the interconnection between dismantling and depollution.

126 2.3.1 Methods

127 Dismantling is performed manually, semi-automatically (hybrid), or fully automatically (Elwert
128 et al. 2018, Harper et al. 2019, Steinbild 2017). Manual disassembly is limited due to

129 economical and safety aspects. Hybrid concepts combine manual activities with industrial
130 robots. Fully automated approaches use only industrial robots. The latter are in the focus of
131 current interest and research (Ay et al. 2012, Harper et al. 2019, Treffer 2011, Zhao 2017a).
132 Generally, disassembly is an economic optimization problem between the dismantling depth,
133 and the costs for the equipment and operating expenditure (Harper et al. 2019). Therein, the
134 dismantling depth is a qualitative measure to describe the progress of disassembly in terms of
135 generated parts, components, or its respective status (Nickel 1996). Typical dismantling depths
136 are battery system, module, cell or electrode level. Additionally, the feed material for a
137 dismantling step represents the lowest dismantling depth being increased by disassembly.

138 2.3.2 Opening of battery cells

139 Cell opening breaks up the battery cells' housings to enable the separation of the individual
140 components (Schubert 2002). It is part of the dismantling or liberation step (Werner et al. 2020)
141 and presents an additional optimisation tasks of dismantling depth and mechanical and/or
142 metallurgical processing (Marshall et al. 2020, Nickel 1996). The methods for cell opening are
143 distinguished in manual or automatic procedures. Chipping in combination with disassembling
144 is applied manually, whereas severing automatically. This contribution assigns chipping in
145 combination with disassembling as manual cell opening within the unit operation dismantling.
146 In contrast to that, automatic severing complies with mechanical cell opening similar to
147 crushing/shredding and is therefore part of the unit operation liberation.

148 Chipping is done with geometrically determinate or indeterminate cutting edges in order to
149 open the housing of battery cells. Metal and diamond saws, water or laser beams can be used
150 for this purpose as well. However, using diamond saws and laser beams is very time consuming,
151 lacks efficiency and causes fire hazard (Zhao 2017b). After chipping, the functional unit is
152 removed manually. The following disassembly of the functional unit into its individual
153 components is carried out manually as well.

154 2.3.3 Chipping in combination with disassembling

155 The combination of chipping with disassembling is known as “direct recycling route” (Chen et
156 al. 2019), “full component recovery strategy” (Zhao 2017a) or „full component recycling
157 process“ (Zhao et al. 2019). This approach is applied to recover the active material of the
158 electrodes for the investigation of metallurgical, especially hydrometallurgical, refining
159 treatment. This reverse engineering approach theoretically achieves the maximum RE.
160 However, it is not industrially applied yet due to high personal effort and low throughput rates
161 for consumer batteries in particular (c.f. 2.2.1). Altogether, specific procedures and processing
162 times, especially for traction batteries, are rare in literature (Arnberger et al. 2018, Cerdas et al.
163 2018, Weyhe et al. 2016).

164 2.4 Depollution

165 The unit operation depollution prevents carry-over of critical or hazardous components or
166 material conditions into subsequent process steps. In addition, depollution avoids the release of
167 harmful emissions into the environment (Martens et al. 2016). The hazard potentials of EOL-
168 LIBs are various: electrical, chemical, and thermal (cf. 2.1.2). Depending on the individual
169 recycling process and its products, the depollution utilizes different methods, such as electrical,
170 cryogenic, and/or thermal treatment, in order to remove hazardous substances or deactivate
171 problematic conditions.

172 2.4.1 Methods and strategies

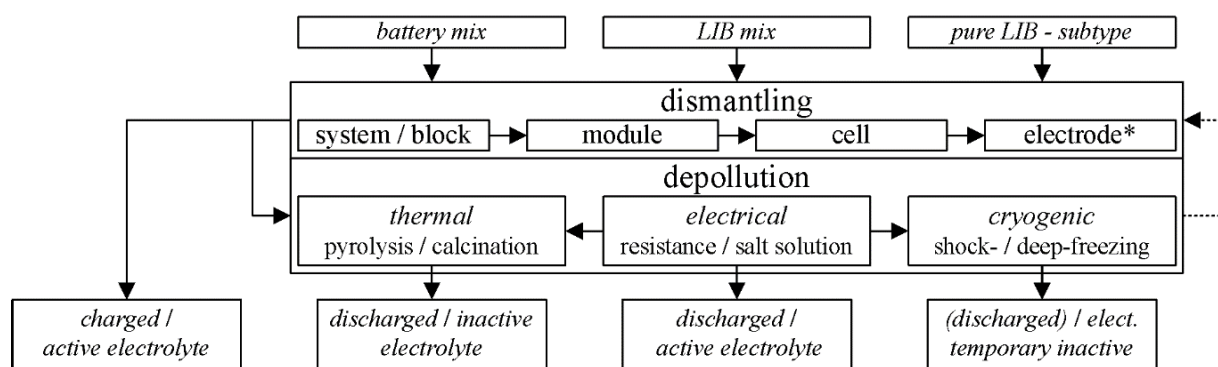
173 Electric and cryogenic treatment can be applied for the low temperature route. Electrical
174 treatment includes mostly discharging to lower the remaining electrochemical potential of the
175 battery (Harper et al. 2019). Therefore, discharging is essential for recycling processes which
176 include dismantling to a high dismantling depth and/or mechanical liberation (Werner et al.
177 2020, Wuschke et al. 2019, Zhao 2017b). Cryogenic treatment avoids exothermic reactions due
178 to the frozen and thus non-conductive electrolyte (Gama 2014). It prevents short circuits and

179 fires. Therein, the batteries are cooled via deep-freezing in liquid nitrogen (Kwade et al. 2018a,
 180 McLaughlin et al. 1999, Pinegar et al. 2019b).

181 Thermal treatment can be distinguished into pyrolysis and/or calcination. Those processes
 182 decompose the electrolyte components by breaking up the organic compounds
 183 thermochemically (Träger et al. 2015, Vezzini 2014). The energy released during this treatment
 184 is used as additional process heat. (Kwade et al. 2018a, Pinegar et al. 2019b, Werner et al.
 185 2020).

186 2.4.2 Material flows

187 The evaluation of hazardous components as well as hazardous conditions depends strongly on
 188 the technological design of the individual recycling routes. Both, components and conditions
 189 influence the requirements and setup of the depollution strategy. Dismantling and depollution
 190 are carried out either downstream or iteratively. Moreover, electrical treatment is applied before
 191 thermal or cryogenic treatment from process technology aspects. Discharging is not necessarily
 192 required, so the latter can also stand-alone. Consequently, various combinations of procedures
 193 are possible, effecting the battery or material properties of the output streams (cf. Figure 1).



195 Figure 1 Dismantling and depollution as part of pre-treatment with potential in- and output
 196 streams, including respective material properties (* single electrodes are not charged (no
 197 electrical depollution necessary) but may still contain electrolyte (remaining chemical hazard
 198 potential)

199 The individual depollution strategy influences the subsequent separation processes. The
 200 depollution of the electrolyte is currently done before or after battery cell opening. After thermal
 201 treatment, the electrolyte is harmless in a subsequent cell opening (Weyhe 2008). In addition,

202 no special requirements are necessary for the process medium. Therefore, most of the industrial
203 applications for LIB recycling use high temperatures to remove these pollutants. However, an
204 appropriate exhaust gas treatment has to be added downstream and the theoretical RE is
205 consequently reduced (Sojka 2020).

206 In contrast to thermal treatment before cell opening, various process designs remove the organic
207 solvents and conducting salt after cell opening (Kwade et al. 2018a). If the electrolyte has to be
208 recovered for material or energetic reuse, only temperatures below the decomposition
209 temperatures of the plastics and electrolyte components are to be applied in the process design
210 (low temperature route). Consequently, the highest theoretical RE can be reached only by three
211 designs: discharging prior to cell opening (1), cell opening in ambient air with simultaneous
212 solvent extraction (2) or using protective atmosphere with subsequent solvent separation (3)
213 (Kwade et al. 2018a, Wuschke et al. 2015). Sojka (2020) presents a detailed but controversial
214 and only qualitatively discussed overview of several process combinations with different
215 depollution strategies and respective RE.

216 2.4.3 Process medium

217 For cell opening, the choice of process medium depends heavily on the hazard potential and
218 depollution status of the feed material. An adequate process medium is often mentioned to
219 design a safe cell opening process (Kwade et al. 2018a). This medium prevents easily and
220 reliably explosive conditions with respect to lower and upper explosive limits (Stehmann et al.
221 2018). Therein, the high variation of feed composition remains a major challenge for a safe cell
222 opening (cf. 2.1.2) accompanied by the differences in depollution status.

223 Besides aqueous media, other wet and also dry process media have been used to reduce the
224 hazard potentials of LIBs during cell opening. On the one hand dry process media are used as
225 protective gases such as argon (Fedjar et al. 2010, Valio 2017), carbon dioxide (Valio 2017),
226 nitrogen (Steinbild 2017) or helium (Gama 2014). Besides of that, ambient air is used as process
227 medium avoiding the explosions limits. The aim is to dilute and remove the liberated solvents.

228 Some of those applications operate at low air throughput using standard dedusting equipment.
229 Other concepts use high throughputs generated by respective ventilators (Wuschke 2018).
230 Finally, salt solutions are used as process medium (Valio 2017) containing calcium or
231 magnesium (Woehrle et al. 2011).

232 3 Materials and methods

233 Manual cell opening and subsequent separation of organic solvents are examined and compared
234 in this contribution. The temperatures for solvent separation during thermal depollution are
235 selected in such a way that the plastics and electrolyte components are at maximum decomposed
236 to a very small extent. Higher temperatures for battery depollution were examined by Weyhe
237 (2008) as well as Weyhe et al. (2016). As a result, the influence of thermal depollution and
238 dismantling depth on solvent release can be determined quantitatively and qualitatively.

239 The latter is seen as ideal procedure for component and subsequent material separation in
240 comparison to mechanical liberation and separation. Consequently, the mass recovery of
241 volatile organic solvents can be evaluated for the respective dismantling depths and manual cell
242 opening method. Also, the distribution of solvents among the different solid components of a
243 battery cell can be quantified. Hence, the method of manual cell opening allows an analytical
244 determination of LIB composition and gives a reference of organic solvent vaporization during
245 mechanical liberation.

246 3.1 Materials

247 A prismatic hard case LIB cell type (170 x 45 x 135 mm) is used due to its state-of-the-art
248 status, current focus of interest, and its poor energy utilization, i.e. highest electrolyte content
249 compared to the other cell types (Hettesheimer et al. 2017). The individual LIB cells origin
250 from an automotive battery system consisting of 8 modules with 12 cells each (Weyhe et al.
251 2016). The burst membrane between the electrical poles of each cell shows a rectangular shape
252 with 36 x 12 mm.

253 Table 1 shows the material composition of these battery cells determined by manual
 254 disassembly and separation. However, only qualitative data and the overall share for the
 255 solvents are available for the electrolyte since the amount of solvents was unknown and had to
 256 be determined by vacuum drying. The solvent consisted of DMC, EMC and DEC as highly
 257 volatile components, and EC as lowly volatile ingredient. The conductive salt and additives
 258 remain theoretically within the pores of the other cell components.

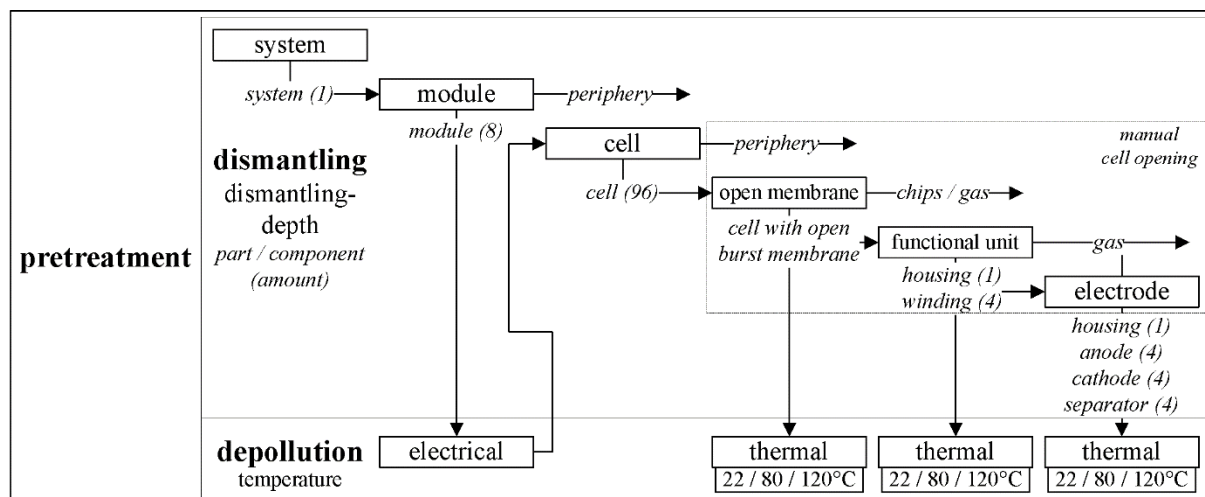
component	function	material	w in %
cathode	metal foil	aluminium	3.0
	coating	NMC + PVDF + additives	34.0
	metal foil	copper	7.2
anode	coating	graphite + SBR + CMC + additives	17.9
	NSD contact	copper	0.9
	electrical contact	copper	0.7
	electrical contact	aluminium	0.3
	case	aluminium	11.8
housing	retainer	PP	0.7
	sleeve	PET	0.3
	NSD foil	PP	0.1
	foils	PP	0.2
	glue		0.2
	others		0.5
separator	foil	PP/PE/PP	1.9
		DMC	
electrolyte	organic solvents	EMC	16.8
		DEC	
		EC	
	conductive salt additives	LiPF6	2.6
			1.0

259 Table 1 material composition of the used battery cells

260 3.2 Experiments

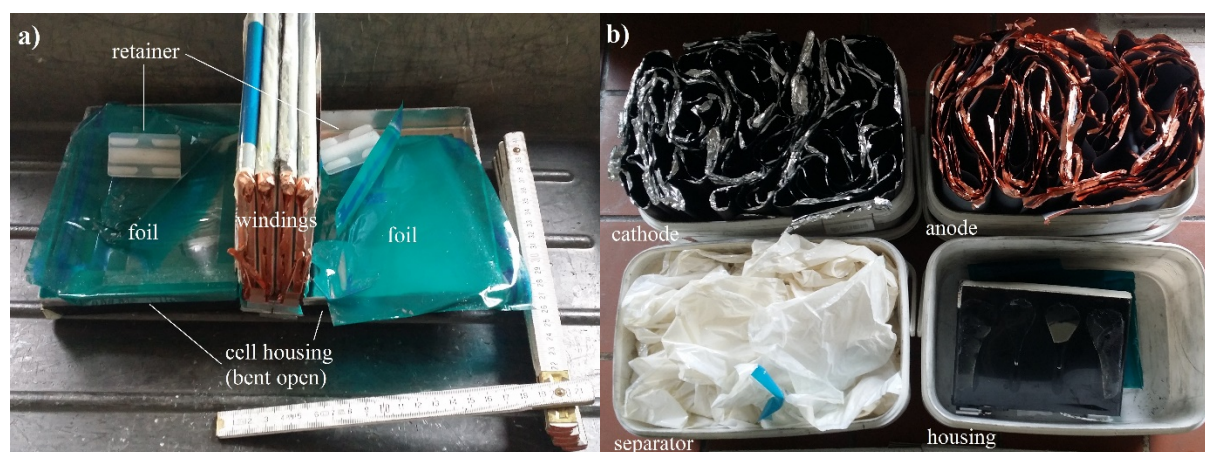
261 Complex and multistep experiments in laboratory scale were employed, combining dismantling
 262 and depollution (cf. Figure 2). Dismantling of a battery system (*system*) to module and cell level
 263 was carried out via manual disassembling, using several tools to liberate the different
 264 components. Electrical depollution was performed at module level with an electrical resistance.
 265 Afterwards, the cells were opened manually in normal air. The burst membrane was grooved
 266 with a common slotted screwdriver (Figure 2: *open membrane*). The cell housing was opened

267 with a 300 mm hacksaw cutting the three smallest side panels of the prismatic cells, which did
 268 not contain the electrical poles. Then, the housing was bent open and the electrical contacts
 269 were removed to detach four windings (c.f. Figure 3 left) using a common pipe wrench.



270
 271 Figure 2 Flow chart of experimental procedure

272 The protection foils were manually pulled of each winding (Figure 2: *functional unit*) and were
 273 added to the housing components (Figure 2: *housing*; c.f. Figure 3 middle). Finally, the
 274 windings were unrolled and *anode*, *cathode* and *separator* were separated manually as well (c.f.
 275 Figure 3 right). The mass of the individual components as well as the time for each dismantling
 276 step were recorded.



277
 278 Figure 3 Manually opened prismatic hard case LIB cell: a) cell housing bent open after
 279 chipping; b) separated cell components with empty cell housing in closed position and
 280 unrolled components of functional unit (four windings from a))

281 The organic solvents were evaporated for cells with open valve, the functional units and the
 282 electrodes via thermal drying under ambient atmosphere. Therefore, a laboratory fume under

283 room temperature (ca. 22 °C) and two laboratory drying chambers (HERAEUS t 6420 for 80 °C
284 and MEMMERT universal oven UF 110 for 120 °C) were used. Three temperatures (22 °C,
285 80 °C, 120 °C) and two drying times (1 h, 120h) were set for solvent evaporation representing
286 the immediate as well as a long term release. The selection is based on studies in literature (He
287 et al. 2015, Pinegar et al. 2019a, Stehmann et al. 2018, Wang et al. 2016, Zhang et al. 2015)
288 and the melting temperature of the separators' plastics, which should not be exceeded. The
289 numbers in brackets in Figure 2 represent the amount of parts or cells disassembled from *system*
290 to *cell* level. The ones for the dismantling depth *functional unit* and *electrodes* represents the
291 components after the *cell* was manually opened. Three cells were investigated for each
292 depollution temperature of the respective dismantling depth. Thus, in total 27 cells were
293 prepared for the experiments.

294 3.3 Methods

295 The processes of dismantling and thermal drying are analysed by the mass balance in respect
296 to the influence of different pre-treatment strategies. Therefore, the in- and output mass m_i and
297 m_o of individual materials (cell, cell with burst membrane open and winding) and components
298 (housing, anode, cathode, and separator) as well as the time spent for the respective process
299 step was determined. With that, the throughput of manual dismantling \dot{m} could be determined
300 as relation of feed mass and processing time. If several dismantling steps were carried out, the
301 output mass of the first step equals the feed mass for the following one.

$$\dot{m} = m_i / t_r \quad (1)$$

302 The mass difference between in- and output mass is associated either to solid parts of the battery
303 system and module periphery or gases from evaporating organic solvents or their respective
304 decomposition products. The amount of dust or small fragments like chips is negligible. The
305 relative mass difference Δw is related to the cell mass representing in general only evaporated
306 solvents.

$$\Delta w = (m_i - m_o) / m_{\text{cell}} \quad (2)$$

307 In contrast, the relative amount w_{os} of organic solvent for one of the cells components j
 308 (housing, anode, cathode, and separator) is calculated by the evaporated mass of each
 309 component j in relation to the overall evaporated mass of solvents at the respective temperature.

$$w_{\text{os},j} = (m_{i,j} - m_{o,j}) / (m_i - m_o) \quad (3)$$

310 The mass reduction of solvents equals the recovery of solvents in the theoretical solvent
 311 fraction $\Delta w_{\text{os},j}$. This fraction represents the total amount of solvents evaporated from a
 312 component and is determined by the product of mass recovery R_m at the respective temperature
 313 and each component's mass reduction of organic solvents $w_{\text{os},j}$ in relation to the cell's organic
 314 solvent content $w_{\text{os},\text{cell}}$.

$$R_m = m_{\text{material fraction}} / m_i \quad (4)$$

$$\Delta w_{\text{os},j} = R_{\text{os},j} = R_m \cdot w_{\text{os},j} / w_{\text{os},\text{cell}} \quad (5)$$

315 Often, the mean value (MV) as well as minimum (MIN) and maximum (MAX) will be
 316 highlighted for a better overview.

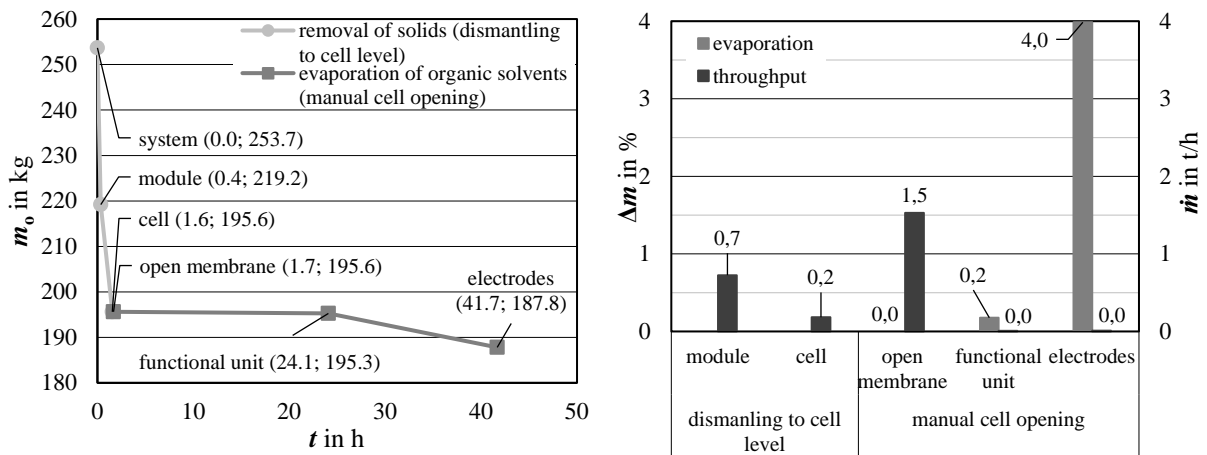
317 4 Results and discussion

318 4.1 Dismantling and manual cell opening

319 Each dismantling step is accompanied by a certain decrease of remaining mass m_o due to
 320 removal of solid and gas components (cf. Figure 4 left). The solid components consist of system
 321 and module peripheral parts like system and module housing, battery management system,
 322 thermal regulation system, electronics and electrical wires and connectors. These components
 323 can be fed into already established recycling routes benefiting the recycling efficiency of the
 324 battery itself. The gases correspond to the evaporated organic solvents contained in the
 325 electrolyte, which are volatilized during cell opening or its decomposition products. Process
 326 time and dismantling costs increase with increasing dismantling depth since more components
 327 and compounds have to be treated individually. Especially, manual chipping and unrolling the

328 electrode stacks are time-consuming processes (Wuschke 2018). As a result, the throughput of
 329 such a process decreases with increasing dismantling depth of manual cell opening (cf. Figure
 330 4 right).

331 The disassembly of battery systems to modules or cells generates only solid components. The
 332 share of chips generated by hacksawing the cell housing is negligible ($< 0.01\%$). Comparing
 333 the different dismantling depths, dismantling to electrode level shows the maximum possible
 334 mass reduction for subsequent mechanical processing and the most efficient evaporation of the
 335 solvent due to tremendously enlarged surface area.



336 Figure 4 left) output mass and process time for different dismantling steps; right) influence of
 337 process step on mass reduction by evaporation and on possible throughput for the respective
 338 dismantling step

339 From a design point of view, the individual windings of the battery type investigated are almost
 340 completely enclosed by an additional plastic foil (c.f. Figure 3 left and middle). With that, the
 341 electrolyte cannot be released from the pores of the coating materials and the separator during
 342 dismantling. Only small amounts of solvent evaporate at ambient conditions if the burst
 343 membrane or the housing is opened. In contrary to that, dismantling to electrodes level increases
 344 the volatilization of solvents. That may be equated with the uncontrolled stressing by arbitrary
 345 tools, which damages usually the functional unit or liberates partially or completely its
 346 components.

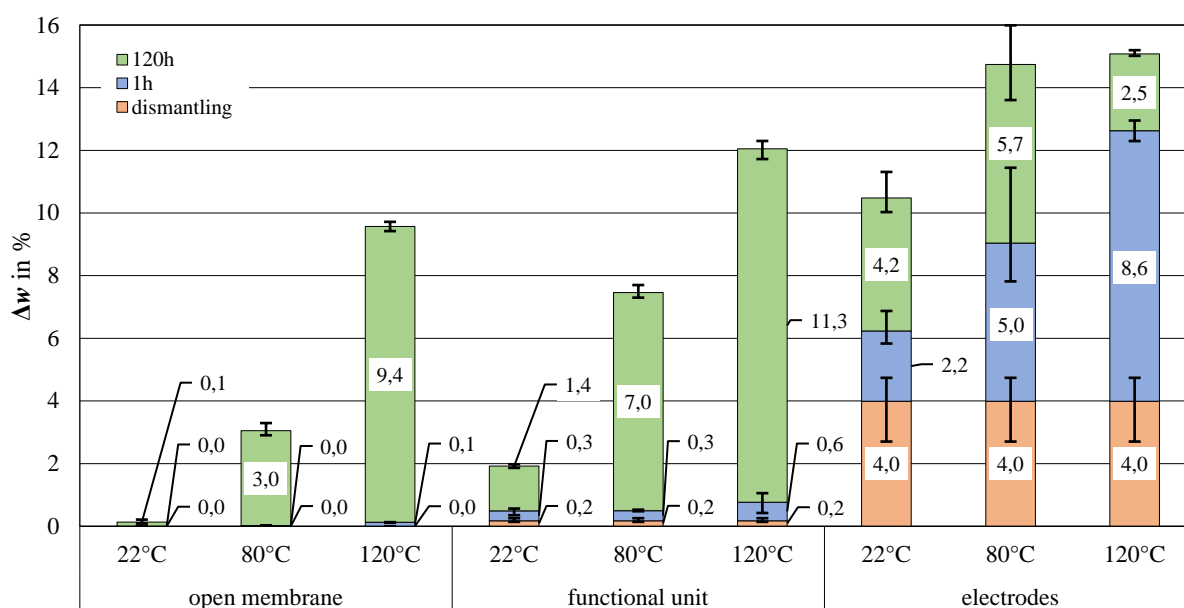
347 Solvent removal represents the reverse process of electrolyte filling within cell production.
348 During cell production, electrolyte filling is the most time-consuming sub-process. Therefore,
349 pressure and temperature are already optimized in this field (Knoche et al. 2016). Consequently
350 within recycling, solvent removal takes quite long as well. Most of the solvents appear to be
351 contained inside of the pores and only a small proportion on the outside of the plastic foil.
352 In principle, the evaporation of solvents increases with increasing dismantling depth. As soon
353 as the functional unit is partially liberated, more components and more mass of solvent
354 volatilize due to a larger free or active surface area. Especially low boiling solvents like DMC,
355 DEC and EMC are emitted in the initial steps generating a hazardous, i.e. explosion
356 potential (Stehmann et al. 2018). Therefore, cell opening has to comply with the explosion
357 limits of such a mixture to provide safe operation conditions.

358 4.2 Depollution

359 Thermal depollution of the LIBs at different dismantling depths was examined for three
360 temperatures and two drying times. Naturally, the mass due to evaporation increases with higher
361 temperature and longer drying times. If the previous dismantling is taken into account, the
362 cumulative mass difference depends also on the surface area (cf. Figure 5). Therefore, the
363 functional unit and especially the components on electrodes level show a faster drying kinetic
364 compared to the case of the opened burst membrane. Within the first hour of drying, a big share
365 of solvents is already evaporated, even increasing with higher temperatures.

366 Cells with open burst membrane and the functional units show the biggest effect of evaporation
367 between 1 and 120 hours due to different heat and mass transfer through the materials. As a
368 result, only high surface area, long drying time and high temperatures separate the volatile
369 electrolyte components to a sufficient degree. Otherwise, especially the organic solvents with
370 high boiling point remain in the cell or cell components. Stehmann et al. (2018) stated that if
371 the temperature is the main driver for solvent removal via thermal drying, information on the
372 boiling temperature of the solvents contained is required to estimate the drying potential. Since

373 the electrolyte is a solvent mixture, the relative volatility of the organic components determines
 374 the drying efficiency. Especially the low volatile solvents tend to remain with the solids, either
 375 adsorbed or still as liquid phase within the porous structure of the materials. It is supposed that
 376 with increasing drying temperature the solvent removal becomes more and more complete. In
 377 order to separate the low volatile solvents, the drying temperature has to be adjusted or rather
 378 increased (Sattler 2001, Stehmann et al. 2018).



379 Figure 5 Influence of drying temperature and time on mass difference for different
 380 dismantling depths
 381

382 Figure 6 shows the cumulative reduction of organic solvent over all steps during thermal
 383 depollution after 120 hours drying time for the individual cell components as well as the overall
 384 pretreatment of electrodes, consisting of the process chain from manual cell opening to
 385 depollution (cf. 3.2). The majority of the organic solvents are on the surface as well as in the
 386 pores of the components. The housing and its plastic foils show only small amounts of
 387 superficial solvents, so the corresponding mass reduction is hardly measurable and negligible.
 388 Irrespective to the temperature used, the mass reduction of organic solvents increases with
 389 increasing material thickness and pore volume of the components. With respect to the organic
 390 solvent content measured at electrode level, more than 90 % of solvents are already removed

391 during dismantling and drying at 120 °C. The relative amount of organic solvents evaporating
 392 from the individual cell components is independent on the temperature (cf. Table 2).
 393 The results of thermally treating the components at electrodes level at 22 °C indicate that around
 394 10 % of the cell representing 63 % of the total solvent content consists of low boiling
 395 components DMC, EMC and DEC. If the temperatures are raised, the evaporation kinetics of
 396 the low boiling solvents is increasing and, in addition, the high boiling components start to
 397 evaporate, even the total relative mass difference between 80 °C and 120 °C at 120°h remains
 398 equal. However, the used temperatures or residence times are not sufficient in order to evaporate
 399 the high boiling solvent EC, which has to make up the other 37 % of the total solvent content.
 400 According to Yang et al. (2006), no conductive salt decomposes, as long as solvents are in
 401 presence. Hence, no hydrofluoric acid (HF) is created during the used thermal treatment setup.

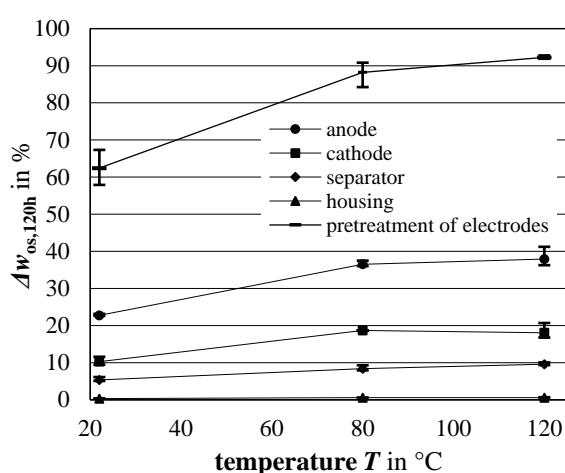


Figure 6 Influence of drying temperature on reduction of organic solvents with respect to amount of organic solvents in the component (MV; MIN; MAX)

component	temperature T in °C	organic solvent share w _{os,120h} in %		
		MV	MIN	MAX
anode	22°C	58,8	58,4	59,4
	80°C	56,9	56,1	57,7
	120°C	57,3	54,8	59,8
cathode	22°C	26,6	24,4	27,8
	80°C	29,1	29,1	29,1
	120°C	27,3	25,3	29,3
separator	22°C	13,8	13,1	15,1
	80°C	13,1	12,4	13,8
	120°C	14,5	14,1	14,9
housing	22°C	0,9	0,7	1,0
	80°C	0,9	0,8	1,0
	120°C	0,9	0,7	1,0

Table 2 Influence of drying temperature on the share of organic solvents in the individual cell components measured at electrode dismantling level after 120 h drying

402 4.3 Proposal of a recycling chain

403 Dismantling LIBs to functional unit or electrodes level simplifies or even dispenses further
 404 sorting steps due to the removal of the housing components. Unfortunately, the necessary
 405 manual dismantling consumes time and labour force, which makes it economically unfeasible.
 406 Therefore, automated dismantling or mechanical processing incorporating crushing is the most
 407 promising approach. Both of them have to adopt the challenges coming from the high variety

408 of LIB (c.f. 2.2.1 and 2.3). Their complexity in design and material compositions increases with
409 the ever-growing variety of applications and special requirements of LIB, especially for
410 automotive applications with respect to fast charging and high range. The variety of cell
411 compounds differs from modular and easily demountable to agglutinated throwaway types with
412 a multitude of different dimensions and designs.

413 Thermal depollution of LIBs with open burst membranes can theoretically skip discharging and
414 avoids a protective atmosphere during cell opening (Pinegar et al. 2020). This results in a less
415 complex design of process technology as well as economic benefits regarding capital and
416 operational expenditure. However, this approach shows disadvantages like a long process time
417 and insufficient solvent removal. The necessary energetic input and expenditure of time for
418 solvent removal does not outweigh the benefit of a simplified subsequent separation of the
419 remaining solid materials and an increased recycling efficiency. Furthermore, pre-sorting is
420 necessary regarding cells with an easily accessible and openable burst membrane. Opening cells
421 without a burst membrane by methods like drilling or sawing gives access to the functional
422 units, but require additional safety measures. In this case, solvent removal will be similar to the
423 methods described in this investigation. As a consequence, only temperatures at or above
424 250 °C present a feasible option as an adequate depollution strategy for all cell types. The so
425 called moderate temperature route causes cell disruption by the increased inner pressure of the
426 cell during thermal depollution, but is only accompanied by a limited recycling efficiency
427 (Sojka 2020, Weyhe et al. 2016).

428 The amount of removed solvents increase with the dismantling depth due to higher surface area
429 for thermal depolluted functional units or electrodes. It therefore remains doubtful from a
430 thermodynamic perspective whether all solvents can be separated at ambient conditions, as
431 especially high boiling solvents require higher temperatures or lower pressure in order to
432 evaporate. Regarding process designs, if recycling technologies avoid a drying step or apply a
433 drying step only at ambient conditions after cell opening, they have to deal with further

434 continuous solvent evaporation in the subsequent physical separation or metallurgical refining
435 processes. The solvents will basically contaminate all generated material fractions, whereby the
436 housing fraction only in small amounts. Moreover, processing wet materials is not desirable
437 (Diekmann et al. 2018), and enclosure of the processing equipment is expensive and
438 complicates maintenance work.

439 5 Conclusion

440 LIBs have several hazard potentials, which have to be deactivated for the safe processing of
441 EOL material. The hazard potentials originating from the organic solvents of EOL-LIB are
442 currently deactivated cryogenically or with high temperatures before cell opening. The latter is
443 applied in particular on industrial scale at the high or the moderate temperature route.
444 Alternatively at low temperature routes, the organic solvents have to be separated after cell
445 opening. The interdependence of dismantling and depollution during the pretreatment of EOL-
446 LIB have been examined in order to determine their influence on solvent extraction. Within this
447 scope, different recycling chains have been tested and discussed.

448 In general, the evaporation of organic solvents increases with increasing dismantling depth,
449 temperature and time for (thermal) drying. Dismantling to electrode level evaporates already
450 around 25 mass percentage of the contained solvents increasing the drying kinetics due to higher
451 surface area. The mass loss can be mostly correlated to the evaporation of the low volatile
452 organic solvents. Also, the highest share of solvents evaporates directly from the surface and
453 the pores of the anode, followed by the pores of the cathode and separator. Within that, the
454 temperature does not influence the relative amount of evaporated solvents. Therefore, the
455 evaporation kinetics are influenced more by morphological features of the cell components
456 instead of the drying temperature and regime.

457 The investigated opening of the burst membrane and subsequent thermal treatment of the
458 battery cells show no satisfying results regarding solvent removal and process time. It is also

459 only applicable for cells with burst membrane, which requires additional pre-sorting. Therefore,
460 safety measures have to be envisioned, if the solvents are separated either directly at or after
461 cell opening. These options have to be applied in particular for pouch and round cells
462 independent of their size and mass. For those cells can be expected that the solvent release
463 during cell opening is lower compared to prismatic cells due to higher energy utilization.

464 Manual cell opening and dismantling to electrodes level simplifies further material separation,
465 but is a time consuming, and thus an uneconomic process (Pinegar et al. 2020). Furthermore, it
466 lacks to scale-up for the increasing variety of battery geometries and types (Wang et al. 2016).
467 Therefore, dismantling to cell or even module level only are more realistic scenarios for high-
468 throughputs in industrial applications.

469 In general, the safe cell opening depends on the batteries' state-of-charge and health, the
470 deactivation status of flammable organic solvents. If RE has to be maximized, plastics,
471 electrolyte, graphite and Al have to be recovered additionally to Cu, Li metal oxides and steel.
472 Thus, discharging is essential for cell opening and the solvents have to be extracted at
473 temperatures at which the conductive salt and plastics do not decompose. The further separation
474 of the solvents into their respective components after extraction from the batteries remains an
475 unsolved task.

476 Several industrial applications are available worldwide providing secondary raw materials for
477 battery applications or other products. One concept is the direct reuse of cathode active
478 materials for new batteries (Shi et al. 2018). However, this reuse is not yet proven to be feasible
479 with the continuous development of battery technology so far (Larouche et al. 2020).
480 Alternatively, the design for recycling could be promoted enhancing the manual or even
481 automatic dismantling and discharging of the batteries. However, cell opening and separation
482 of the individual components remain the bottlenecks for automation from a manufacturing
483 processing point of view (Marshall et al. 2020).

484 **Acknowledgements**

485 The authors gratefully like to acknowledge the BMW AG which provided materials and
486 information for the experimental part. The authors also like to thank the technical and scientific
487 stuff of the Institute of Mechanical Process Engineering and Mineral Processing for making the
488 equipment used for the experimental part available.

489 **Contribution**

490 D.M.W. designed and carried out the experiments. D.M.W. prepared the manuscript and
491 analysed the data integrating contributions from T.M. and U.A.P. T. M. and U.A.P. critically
492 reviewed the work, the former multiple times.

493 **Funding:**

494 The authors like to thank the Federal Ministry for Education and Research (BMBF) as well as
495 the Projektträger Jülich (PTJ) for funding the project “Innovative Recyclingprozesse für neue
496 Lithium-Zellgenerationen - Mechanische Prozesse” (InnoRec) within the Competence cluster
497 for battery cell production (ProZell).

498 **Conflicts of Interest:**

499 The authors declare no conflict of interest.

500 **6 References**

- 501 Arnberger A, Coskun E and Rutrecht B (2018) *Recycling von Lithium-Ionen-Batterien*. in: K.J. Thomé-
502 Kozmiensky, D. Goldmann (Eds.), *Recycling und Rohstoffe*, Neuruppin, 583-599.
- 503 Arnberger A, Gresslehner K-H, Pomberger R and Curtis A (2012) *Recycling von Lithium Ionen Batterien aus*
504 *EVs & HEVs. DepoTech 2012*, Leoben, AT, 6 November 2012.
- 505 Ay P, Markowski J, Pempel H and Müller M (2012) *Entwicklung eines innovativen Verfahrens zur*
506 *automatisierten Demontage und Aufbereitung von Lithium-Ionen-Batterien aus Fahrzeugen. Recycling und*
507 *Rohstoffe 5*: 443-456.
- 508 Cerdas F, Gerbers R, Andrew S, Schmitt J, Dietrich F, Thiede S, Dröder K and Herrmann C (2018) *Disassembly*
509 *Planning and Assessment of Automation Potentials for Lithium-Ion Batteries*. in: A. Kwade, J. Diekmann
510 (Eds.), *Recycling of Lithium-Ion Batteries - The LithoRec Way*, New York, NY, USA, 83-97.
- 511 Chen M, Ma X, Chen B, Arsenault R, Karlson P, Simon N and Wang Y (2019) *Recycling End-of-Life Electric*
512 *Vehicle Lithium-Ion Batteries. Joule 3(11)*: 2622-2646. <https://doi.org/10.1016/j.joule.2019.09.014>.
- 513 Diekmann J, Sander S, Sellin G and Kwade A (2018) *Material Separation*. in: A. Kwade, J. Diekmann (Eds.),
514 *Recycling of Lithium-Ion Batteries - The LithoRec Way*, New York, NY, USA, 207-217.
- 515 Elwert T, Römer F, Schneider K, Hua Q and Buchert M (2018) *Recycling of Batteries from Electric Vehicles*. in:
516 G. Pistoia, B. Liaw (Eds.), *Behaviour of Lithium-Ion Batteries in Electric Vehicles - Battery Health,*
517 *Performance, Safety, and Cost*, Cham, Switzerland.
- 518 Fedjar F and Foudraz J-C (2010) *METHOD FOR THE MIXED RECYCLING OF LITHIUM-BASED ANODE*
519 *BATTERIES AND CELLS*.
- 520 Gaines L, Sullivan J and Burnham A (2011) *Life-Cycle Analysis for Lithium-Ion Battery Production and*
521 *Recycling. 90th Annual Meeting of the Transportation Research Board*, Washington, D.C.
- 522 Gama M (2014) *European Li-Ion Battery Advanced Manufacturing For Electric Vehicles - ELIBAMA*. online

523 Georgi-Maschler T, Friedrich B, Weyhe R, Heegn H and Rutz M (2012) Development of a recycling process
524 for Li-ion batteries. *Journal of Power Sources* 207: 173-182.

525 Hanisch C, Diekmann J, Stieger A, Haselrieder W and Kwade A (2015) *Recycling of Lithium-Ion Batteries*. in: J.
526 Yan, L.F. Cabeza, R. Sioshansi (Eds.), Handbook of Clean Energy Systems, Hoboken, NJ, USA, 2865-2888.

527 Harper G, Sommerville R, Kendrick E, Driscoll L, Slater P, Stolkin R, Walton A, Christensen P, Heidrich O,
528 Lambert S, Abbott A, Ryder K, Gaines L and Anderson P (2019) Recycling lithium-ion batteries from
529 electric vehicles. *Nature* 575: 75-86. <https://doi.org/10.1038/s41586-019-1682-5>.

530 He L-P, Sun S-Y, Song X-F and Yu J-G (2015) Recovery of cathode materials and Al from spent lithium-ion
531 batteries by ultrasonic cleaning. 46: 523–528. <https://doi.org/10.1016/j.wasman.2015.08.035>.

532 Hettesheimer T, Thielmann A, Neef N, Möller K-C, Wolter M, Lorentz V, Gepp M, Wenger M, Prill T, Zausch
533 J, Kitzler P, Montnacher J, Miller M, Hagen M and Fanz P (2017) *ENTWICKLUNGSPERSPEKTIVEN FÜR
534 ZELLFORMATE VON LITHIUM-IONENBATTERIEN IN DER ELEKTROMOBILITÄT*. Fraunhofer-Institut
535 für System- und Innovationsforschung ISI. Karlsruhe

536 Idjis H, Attias D, Bocquet J-C and Sophie R (2013) Designing a Sustainable Recycling Network for Batteries
537 from Electric Vehicles. Development and Optimization of Scenarios. *14th Working Conference on Virtual
538 Enterprises*, Dresden, Germany, 30 September–2 October 2013, 609 - 618.

539 Knoche T, Surek F and Reinhart G (2016) A process model for the electrolyte filling of lithium-ion batteries.
540 *48th CIRP Conference on MANUFACTURING SYSTEMS - CIRP CMS 2015*, Ischia, Italy, 24-26.06.2015.

541 Korthauer R (2013) *Handbuch Lithium-Ionen-Batterien*. Berlin Heidelberg.

542 Korthauer R (2019) *Lithium-Ion Batteries: Basics and Applications*. Berlin, Germany.

543 Kwade A and Diekmann J (2018a) *Recycling of Lithium-Ion Batteries - The LithoRec Way*. New York, NY,
544 USA.

545 Kwade A, Haselrieder W, Leithoff R, Modlinger A, Dietrich F and Droeder K (2018b) Current status and
546 challenges for automotive battery production technologies. *Nature Energy* 3: 290–300.

547 Larouche F, Tedjar F, Amouzegar K, Houlachi G, Bouchard P, Demopoulos GP and Zaghbi K (2020) Progress
548 and Status of Hydrometallurgical and Direct Recycling of Li-Ion Batteries and Beyond. *Materials* 13
549 <https://doi.org/10.3390/ma13030801>.

550 Li L, Zheng P, Yang T, Sturges R, ELLIS MW and Li Z (2019) Disassembly Automation for Recycling End-of-
551 Life Lithium-Ion Pouch Cells. *The Journal of The Minerals, Metals & Materials Society* 71(12): 4457-4464.

552 Marshall J, Gastol D, Sommerville R, Middleton B, Goodship V and Kendrick E (2020) Disassembly of Li Ion
553 Cells - Characterization and Safety Considerations of a Recycling Scheme. *Metals* 10(773)
554 <https://doi.org/10.3390/met10060773>.

555 Martens H and Goldmann G (2016) *Recyclingstechnik*. Wiesbaden.

556 McLaughlin W and Adams TS (1999) *LI RECLAMATION PROCESS*.

557 Mossali E, Picone N, Gentilini L, Rodríguez O, Perez JM and Colledani M (2020) Lithium-ion batteries towards
558 circular economy: A literature review of opportunities and issues of recycling treatments. *Journal of
559 Environmental Management* 264 <https://doi.org/10.1016/j.jenvman.2020.110500>.

560 Nickel W (1996) *Recyclinghandbuch: Strategien - Technologien - Produkte*. Düsseldorf.

561 Pinegar H and Smith YR (2019a) End-of-Life Lithium-Ion Battery Component Mechanical Liberation and
562 Separation. *The Journal of The Minerals, Metals & Materials Society* 71(12): 4447-4456.

563 Pinegar H and Smith YR (2019b) Recycling of End-of-Life Lithium Ion Batteries, Part I: Commercial Processes.
564 *Journal of Sustainable Metallurgy* <https://doi.org/10.1007/s40831-019-00235-9>.

565 Pinegar H and Smith YR (2020) Recycling of End-of-Life Lithium-Ion Batteries, Part II: Laboratory-Scale
566 Research Developments in Mechanical, Thermal, and Leaching Treatments. *Journal of Sustainable
567 Metallurgy* <https://doi.org/10.1007/s40831-020-00265-8>.

568 Pomberger P and Ragosnig A (2014) Future waste – waste future. *Waste Management & Research* 32(2): 89–
569 90. <https://doi.org/10.1177/0734242X14521344>.

570 Rahimzei E (2017) *Begleit- und Wirkungsforschung Schaufenster Elektromobilität (BuW) Ergebnisrapier Nr. 37
571 - Sicherheit von Elektrofahrzeugen*. Deutsches Dialog Institut GmbH. Frankfurt am Main

572 Rothermel S, Winter M and Nowak S (2018) *Background*. in: A. Kwade, J. Diekmann (Eds.), *Recycling of
573 Lithium-Ion Batteries - The LithoRec Way*, New York, NY, USA, 1-31.

574 Rudolph A (1999) *Altproduktentsorgung aus betriebswirtschaftlicher Sicht*. Heidelberg.

575 Sattler K (2001) *Thermische Trennverfahren - Grundlagen, Auslegung, Apparate*. Weinheim.

576 Schubert G (2002) Comminution Equipment for Non-Brittle Waste and Scrap. *AUFBEREITUNGSTECHNIK*
577 43(9): 6-23.

578 Schwarz TE, Rübenbauer w, Rutrecht B and Pomberger R (2018) Forecasting Real Disassembly Time of
579 Industrial Batteries based on Virtual MTM-UAS Data. *25th CIRP Life Cycle Engineering (LCE) Conference*,
580 Copenhagen, Denmark, 927–931.

581 Shi Y, Chen G and Chen Z (2018) Effective regeneration of LiCoO₂ from spent lithium-ion batteries: a direct
582 approach towards high-performance active particles. *Green Chemistry* 20: 851–862.
583 <https://doi.org/10.1039/c7gc02831h>.

584 Sojka TR (2020) Sichere Aufbereitung von Lithium-basierten Batterien durch thermische Konditionierung.
585 *Recycling und Sekundärrohstoffe*, Berlin, DE, 506-523.

586 Stehmann F, Bradtmöller C and Scholl S (2018) *Separation of the Electrolyte—Thermal Drying*. in: A. Kwade,
587 J. Diekmann (Eds.), *Recycling of Lithium-Ion Batteries - The LithoRec Way*, New York, NY, USA, 139-
588 153.

589 Steinbild M (2017) *Recycling von Lithium-Ionen-Batterien - LithoRec II: Abschlussbericht der beteiligten*
590 *Verbundpartner*. Bundesministeriums für Umwelt, Naturschutz, Bau und Reaktorsicherheit.

591 Träger T, Friedrich B and Weyhe R (2015) Recovery Concept of Value Metals from Automotive Lithium-Ion
592 Batteries. *Chemie Ingenieur Technik* 87: 1550-1557.

593 Treffer F (2011) *Entwicklung eines realisierbaren Recyclingkonzeptes für die Hochleistungsbatterien*
594 *zukünftiger Elektrofahrzeuge*. Umicore AG & Co. KG. Hanau

595 Tytgat J (2013) The Recycling Efficiency of Li-ion EV batteries according to the European Commission
596 Regulation, and the relation with the End-of-Life Vehicles Directive recycling rate. *International Battery,*
597 *Hybrid and Fuel Cell Electric Vehicle Symposium*, Barcelona, Spain, 17-20.11.2013.

598 Valio J (2017) *Critical Review on Lithium Ion Battery Recycling Technologies*. Master Thesis

599 van Pels W (2020) Herausforderung hinsichtlich der Brandschutztechnologien in Recyclinganlagen insbesondere
600 bei der Verarbeitung von Li-Ionen Traktionsbatterien. *Recycling und Sekundärrohstoffe*, Berlin, Germany,
601 496-505.

602 Vezzini A (2014) *Manufacturers, Materials and Recycling Technologies*. in: G. Pistoia (Ed.) *Lithium-Ion*
603 *Batteries Advances and Applications*, Amsterdam, The Netherlands, 529-551.

604 Wang X, Gaustad G and Babbitt CW (2016) Targeting high value metals in lithium-ion battery recycling via
605 shredding and size-based separation. *Waste Management* 51: 204-213.

606 Wegener K, Andrew S, Raatz A, K. D and Herrmann C (2014) Disassembly of Electric Vehicle Batteries Using
607 the Example of the Audi Q5 Hybrid System. *Conference on Assembly Technologies and Systems*, Dresden,
608 Germany, 15-16.05.2014.

609 Werner D, Peuker UA and Mütze T (2020) Recycling Chain for Spent Lithium-Ion Batteries. *Metals - Open*
610 *Access Metallurgy Journal* 10 (3) (316) <https://doi.org/10.3390/met10030316>

611 Weyhe R (2008) *Verbundprojekt "Rückgewinnung der Rohstoffe aus Li-Ion Akkumulatoren"*. Accurec GmbH.
612 Mühlheim, Germany

613 Weyhe R and Friedrich B (2016) *Demonstrationsanlage für ein kostenneutrales, ressourceneffizientes*
614 *Processing ausgedienter Li-Ionen Batterien aus der Elektromobilität - EcoBatRec - Abschlussbericht zum*
615 *Verbundvorhaben*. IME Metallurgische Prozesstechnik und Metallrecycling. Aachen

616 Woehrle T and Kern R (2011) *Method for performing comminution of battery containing lithium*
617 *hexafluorophosphate used in e.g. vehicle, involves using environmental fluid containing alkaline earth metal*
618 *surrounding the battery for realizing comminution of battery*.

619 Wuschke L (2018) *Mechanische Aufbereitung von Lithium-Ionen-Batteriezellen*. Ph.D. Thesis

620 Wuschke L, Jäckel H-G, Borsdorff D, Werner D, Peuker UA and Gellner M (2016) Zur mechanischen
621 Aufbereitung von Li-Ionen-Batterien. *Berg- und Hüttenmännische Monatshefte* 161(6): 267–276.

622 Wuschke L, Jäckel H-G, Leißner L and Peuker UA (2019) Crushing of large Li-ion battery cells. *Waste*
623 *Management* 85: 317-326.

624 Wuschke L, Jäckel H-G, Peuker UA and Gellner M (2015) Recycling of Li-ion batteries – a challenge. *Recovery*
625 4: 48-59.

626 Yang H, Zhuang GV and Ross Jr. PN (2006) Thermal stability of LiPF₆ salt and Li-ion battery electrolytes
627 containing LiPF₆. *Journal of Power Sources* 161: 573–579. <https://doi.org/10.1016/j.jpowsour.2006.03.058>.

628 Zhang X, Cao H, Xie Y, Ning P, An H, You H and Nawaz F (2015) A closed-loop process for recycling
629 LiNi_{1/3}Co_{1/3}Mn_{1/3}O₂ from the cathode scraps of lithium-ion batteries: Process optimization and kinetics
630 analysis. 150: 186-195. <https://doi.org/10.1016/j.seppur.2015.07.003>.

631 Zhao G (2017a) *Assessment Technology Platform and Its Application for Reuse of Power Batteries*. in: G. Zhao
632 (Ed.) *Reuse and Recycling of Lithium-Ion Power Batteries*, Singapur, 237-260.

633 Zhao G (2017b) *Resource Utilization and Harmless Treatment of Power Batteries*. in: G. Zhao (Ed.) *Reuse and*
634 *Recycling of Lithium-Ion Power Batteries*, Singapur, 335-378.

635 Zhao S, He W and Li G (2019) *Recycling Technology and Principle of Spent Lithium-Ion Battery*. in: L. An
636 (Ed.) *Recycling of Spent Lithium-Ion Batteries - Processing Methods and Environmental Impacts*, Cham, 1-
637 26.

638